SODIUM-IODIDE SYMPORTER EXPRESSION STUDIES IN RED DRUM (*SCIAENOPS OCELLATUS*) TISSUES

An Undergraduate Research Scholars Thesis

by

JULIE MICHELLE BUTLER

Submitted to Honors and Undergraduate Research
Texas A&M University
in partial fulfillment of the requirements for the designation as

UNDERGRADUATE RESEARCH SCHOLAR

Approved by
Research Advisor: Dr. Duncan MacKenzie

May 2013

Major: Biology
Forensic and Investigative Sciences

TABLE OF CONTENTS

Page

ABSTRACT

Sodium-iodide symporter expression studies in red drum (*Sciaenops ocellatus*) tissues.
(May 2013)

Julie Michelle Butler
Department of Biology
Department of Entomology
Texas A&M University

Research Advisor: Dr. Duncan MacKenzie
Department of Biology

Thyroid hormones play crucial roles in regulation of growth, metabolism, reproduction, and other essential physiological processes. In mammals, thyroid hormone synthesis is dependent on uptake of iodine from the blood into thyroid tissue by the sodium-iodide symporter (NIS) protein, with diet being the ultimate iodide source. In contrast, it has been proposed that fish can obtain iodide directly from their environment by pumping it across gills. My study was designed to determine whether fish possess both gill and gut iodide uptake mechanism by characterizing NIS mRNA expression in gill and gut tissues of the red drum. PCR primers for NIS were designed using Clustal X primer design software. Tissue enriched in thyroid follicles located ventral to and between the 2nd and 4th gill arches was collected along with gill and gut for mRNA extraction. NIS was detectable in the thyroid tissue, gill, gut, and brain tissues. Expression in both gill and gut tissues suggests two possible mechanisms of iodide absorption in red drum. NIS expression in the brain is a novel discovery and warrants further studies as to its function and specific location.

ACKNOWLEDGMENTS

Thank you to my research advisor, Dr. Duncan MacKenzie, for all the support, advice, and encouragement he provided me during the duration of this project. Thank you also to Dr. Richard Jones and Dr. Bill Cohn for their support, patience, and guidance throughout this project, as well as Dr. Sunny Scobell for her encouragement.

CHAPTER I

INTRODUCTION

Thyroid hormones are important for many aspects of life in mammalian and non-mammalian species. They play crucial roles in growth, metabolism, reproduction, and other essential physiological processes. Thyroxine (T_4) and triiodothyronine (T_3) are together considered "thyroid hormones" even though T_4 serves as a prohormone to T_3. The difference between the two hormones lies in their structures. T_4 has four iodide atoms whereas, T_3 has only three (Hadley & Levine, 2007). Their structures demonstrate that thyroid hormone synthesis is dependent on the availability of iodide in the thyroid gland. In many animals, iodide is obtained from the diet, absorbed into the bloodstream through the intestine, and transported into the thyroid by the sodium-iodide symporter (NIS) (Nicola et al, 2009; Zimmerman, 2009, Dohan et al., 2003). This protein is located in the basolateral membrane of thyrocytes. Dohan et al. (2003) characterized the protein in humans and rats to have 13 transmembrane regions with an extracellular N-terminus and intracellular C-terminus. The protein works by inward transport of two atoms of sodium and one atom of iodide down a sodium gradient established by a membrane sodium-potassium pump (Ferreira et al, 2010). The activity of NIS is regulated in two ways. The pituitary hormone thyroid stimulating hormone (TSH) acts as a positive regulator promoting synthesis and insertion of more symporters in the membrane to allow for increased iodide uptake. The other regulator is iodide itself. As stored levels of iodide inside the thyroid increase, fewer symporters are present in the membrane, decreasing iodide uptake (Ferreira et al., 2010, Dohan et al, 2003). Therefore, the ability to make T_4 is dependent on precise regulation of protein-mediated transport of iodine uptake across the basolateral membrane.

While the thyroidal iodide uptake mechanism has been characterized for clinically-important mammalian species, almost nothing is known about iodide transport in teleost fish. There are several reasons for this. The first and most prominent reason is that the teleost fish thyroid differs in structure from tetrapod vertebrate classes. The basic functional unit of the thyroid gland throughout vertebrates is the thyroid follicle. In mammals and most other tetrapod species thyroid follicles are grouped together into a discrete encapsulated thyroid gland. However, in teleosts there is no organized collection of follicles; they are instead distributed throughout the lower jaw, pericardium, and anterior kidney (Gorbman et al, 1983). Because of the dispersed thyroid structure it has been difficult to obtain sufficient amounts of thyroid tissue for transporter identification and characterization. The next difference in iodide uptake in fish relates to the ultimate source of iodide. Iodide is abundant in seawater, meaning marine fish are immersed in a constant supply (Kupper et al, 2010). Whereas mammals must ingest iodine through their diet, it has been suggested that teleosts are able to absorb iodine from seawater using a branchial pump in the gills (Higgs et al, 1982). Eales (1979) suggested that this iodide uptake in the gills was part of an excretory process. Hunn and Fromm (1996) noted that the iodide transport mechanism in the gills appeared to resemble the NIS transport mechanism in the mammalian thyroid due to similar sensitivity to inhibitors, but at the present time NIS expression has not been demonstrated in gill tissue. If fish are unable to absorb iodine through their gills, the next most logical location of absorption would be the gut. Many have noted that iodine is an essential mineral for fish nutrition, but no iodide transport protein has been identified in the intestine of teleost fish (Gregory & Eales, 1975; Wantabe et al, 1997; Higgs et al, 1982). Thus it is known that fish obtain iodide from their diet or the environment, but no mechanism has been identified.

The objective of this study is to determine whether an NIS-like protein may be utilized by fish to obtain iodide from their diet and environment. The NIS protein has been sequenced in humans, rats, and mice, as well as several non-mammalian species. Dohan et al (2003) found that the protein sequence is 93% identical between rat and human NIS. They also found that the sequence between mouse, rat, pig, and human NIS was highly conserved. Nicola et al (2008) demonstrated NIS expression in rat and mouse intestine. The gene for NIS has also been sequenced in several teleosts (NCBI accession numbers: Zebra fish: NM_001089391.1, Medaka: JN642280.1, Gobi: FJ624477.1, and Stickleback: FJ773237.1). Carr et al (2008) suggested that NIS gene sequence is structurally conserved among these teleost species. This conservation of sequence suggests that it is possible to clone and characterize NIS in additional fish species to determine whether it is expressed in the gill and gut. To my knowledge, newer molecular tools have not been used to hunt for the NIS in gill and gut tissues.

I propose to apply modern molecular methods of gene sequencing, polymerase chain reactions (PCR) amplification, and gene expression characterization to determine whether a protein homologous to NIS is expressed in fish gill and digestive tract. I propose to do this in red drum, an important research and aquaculture teleost fish species that has been used for thyroid function studies in our laboratory for over 20 years. Red drum are readily available as juveniles from hatcheries as well as from the wild at up to a meter in length, allowing for collection of a large amount of tissue for RNA extraction. Using radioactive iodine-124, recent research in our lab indicated that thyroid tissue is concentrated anterior to the heart (A. Wilkes and Z. Browning, unpublished results). By collecting this region of tissue I hope to extract adequate amounts of thyroid-enriched RNA suitable for identification of the red drum NIS sequence. Finally, we have

recently found that iodine supplementation of food can diminish thyroid insensitivity and TSH stimulation in iodine-depleted water, suggesting iodine transport may be important in supporting growth and metabolism in this species. Insensitive red drum may therefore be an excellent teleost system in which to study the regulation of iodide transport.

CHAPTER II

MATERIALS AND METHODS

Experimental animals

Red drum fingerlings were obtained from the Texas Parks and Wildlife Department Sea Center hatchery in Lake Jackson, Texas, May, 2012. They were kept in artificial seawater ranging from 25-28°C with a 12L:12D photoperiod until they reached at least 50 grams for gill tissue collection and 100 grams for thyroid tissue collection. The artificial seawater was created using reverse osmosis water, Morton salt (IL, USA), and Fritz Super Salt Concentrate (Frtiz Aquatics, TX, USA) to a salinity of 7 ppt. Fish were fed a diet of commercial pellets (Rangen, Angleton, TX) twice daily for the first 3 months and then once daily after that.

Tissue collection

Recent research in our lab using radioactive iodine-124 indicated that thyroid tissue is concentrated in the soft vascularized tissue of the lower jaw between the 2nd and 4th gill arches. To collect this tissue the entire lower jaw was removed including the gill arches. The gill arches were then removed, leaving soft, vascularized tissue. This tissue was expected to contain thyroid follicles and yield enriched amounts of thyroid gland-specific mRNA. Gill tissue was collected by isolating all gill arches with attached gill filaments. Gastrointestinal tract was collected as five separate samples: stomach, pyloric caeca, anterior intestine, medial intestine, and posterior intestine. Opercular membrane tissue was collected by peeling off the interior membrane of the operculum. Operculum (bone included) and brain tissue were also collected. Brain and muscle tissue were collected to serve as negative tissue controls. The collected tissues were snap frozen in liquid nitrogen then homogenized using a mortar and pestle in liquid nitrogen. The mortar and

pestle were stored in the -80°C prior to use so that less liquid nitrogen was needed to cool the mortar and pestle. The resulting frozen tissue homogenate powder was placed in 3 mL of TRIzol reagent (Invitrogen, NY, USA), snap frozen in liquid nitrogen, and stored at -80°C.

RNA extraction

Homogenized tissue in TRIzol reagent was rapidly thawed in a 65°C water bath. A 1ml aliquot was removed and the remainder was snap frozen for future use. The RNA was extracted from the collected tissues following the manufacturer's protocol. The aliquots were incubated for 5 minutes at room temperature (15-20°C) to allow dissociation of the nucleoprotein complexes. After 5 minutes, 0.2mL of chloroform was added to each tube and then each tube was shaken vigorously by hand for 15 seconds. After a 3 minute incubation at room temperature, the samples were centrifuged at 14000rpm for 15 minutes. Centrifugation caused the mixture to separate into a lower red, phenol-chloroform phase, interphase, and a colorless upper phase. The DNA and proteins are found in the interphase and lower organic phase, and the RNA was found in the upper aqueous phase. The upper phase was removed using a sterile pipette and placed into a sterile 1.5mL microcentrifuge tube containing 0.5mL of isopropyl alcohol. The remaining interphase and lower phase were discarded. After a 10 minute incubation at room temperature, the samples were centrifuged at 14000rpm for 10 minutes. The centrifugation caused a small RNA pellet to form at the base of each tube. The supernatant was decanted from each sample into a waste beaker. The pellet was then washed using 0.5mL of 100% ethanol and vortexed. After 5 minutes of centrifugation at 14000rpm, the ethanol was decanted by inversion onto a sterile surface, taking care not to dislodge the pellet. The samples were left to air dry for 5 minutes. To redissolve the pellet, DEPC-treated, autoclaved water was added until the RNA

looked like little glass beads, generally ranging from 80-100µL water depending on the sample size and tissue type.

RNA quantification and gel electrophoresis

RNA samples (1µL) were quantified using Nanodrop technology (Thermo Scientific, Asheville, NC) with ddH_2O as the blank. A 1% gel was made by melting 0.5g agarose in 45mL of ddH_2O. After cooling, 5mL of 10X formaldehyde gel buffer (Ambion, NY, USA) was poured into the cooling agarose solution. The solution was mixed by hand swirling before being poured into the sterilized 8x10 cm gel tray with comb. The gel was left to solidify for 30 minutes at room temperature. After the gel had solidified for 30 minutes it was placed in a sterilized gel box containing 500mL of 1X MOPS running buffer and left to soak for at least 15 minutes while samples were prepared. For gel loading, 5µg of RNA per sample was brought up in 6µL of DEPC-treated autoclaved H_2O and 18µL of RNA loading dye (Ambion, NY, USA). Samples were then vortexed, pulse spun, and placed in a 65°C water bath for 15 minutes. The samples were then pulse spun again, and immediately placed on ice. The comb was removed from the gel and 24µL of sample was carefully loaded in each well. A single-stranded RNA ladder (New England BioLabs, MA, USA) was used for reference. The gel was run at approximately 94 V until the dye front was two thirds of the way down the length of the gel. A staining solution was made by adding 25µL of ethidium bromide to 500mL of ddH_2O in a glass baking dish. The gel was placed in the staining solution and left to gently rock in a shaker for 30 minutes. After 30 minutes, the gel was transferred to 500mL of ddH_2O to destain overnight. The next day the gel was visualized using UV light to ensure that the RNA was not degraded. RNA integrity was determined by the presence of singular, intact ribosomal subunit bands with no smearing.

DNase treatment

All samples were DNase treated prior to reverse transcription using a recombinant DNase I kit (Ambion, NY, USA). For each sample, RNA equal to 2µg was added to 1µL of DNase buffer and 1µL DNase before being QSed to 12µL with DEPC-treated H_2O. This mixture was incubated at 37°C for 30 minutes before 3µL of EDTA was added. It was then incubated in a 70°C water bath for 10 minutes before use in reverse transcription.

Reverse-transcription PCR

Extracted RNA was converted to complementary DNA (cDNA) using a high-capacity cDNA reverse transcription kit (Invitrogen, NY, USA) according to the manufacture's protocol: 5µL 10X RT buffer, 2µL 25X dNTP Mix, 8.0µL 10X RT Random Primers, 2.5µL Oligo dT, RNA equal to 2µg, 2.5µL Reverse Transcriptase, and QSed to 50µL with autoclaved H_2O. The thermocycler conditions were set to 25°C for 10 minutes, 37°C for 120 minutes, 85°C for 5 minutes, and a 4°C hold. All samples were then placed in the -20°C freezer.

Primer design

Clustal X2 for Multiple Sequence Alignment was used for primer design. The NIS primers were based on the following sequences with emphasis placed on teleost sequences: Zebrafish NIS: NM_001089391.1; Medaka (ricefish) NIS partial: JN642280.1; Gobi NIS partial: FJ624477.1; Stickleback NIS partial: FJ773237.1; Tilapia NIS Predicted: XM_003449061.1; Bovine NIS Predicted: XM_581578.6; Canine NIS Predicted: XM_541946.3; Chicken NIS Predicted: XM_429095.3; Chimpanzee NIS Predicted: XM_524154.3; Human NIS: NM_000453.2; Mouse NIS: NM_053248.2; Porcine NIS: NM_214410.1; Rat NIS: NM_052983.2; Frog NIS:

NM_001093422.1; Elephant NIS Predicted: XM_003413265.1; Bonobo NIS Predicted: XM_003817836.1; Panda NIS Predicted: XM_002912722.1; Wolf NIS Predicted: XM_003432897.1; Tasmanian Devil NIS Predicted: XM_003763195.1.

The forward NIS primer was chosen to be ATT$^{C}_{T}$T$^{G}_{C}$AA$^{C}_{T}$CAAG$^{C}_{T}$NACNGG and the reverse NIS primer was GCCATNGC$^{G}_{A}$TT$^{G}_{A}$AT$^{G}_{A}$CTNGT$^{G}_{A}$GA. TSHR primers, designed by Richard Jones as part of his dissertation research, were used as a positive control for PCR. All primers were ordered from Integrated DNA Technologies.

PCR

Each sample for PCR was made using 10µL of GoTaq Green (Promega, WI, USA), 2µL of the RT-reaction from the appropriate tissue, 2µL and 8µL of primer for TSHR and NIS, respectively, and brought up to 20µL with ddH_2O. No-template controls used extra ddH_2O instead of cDNA. Thermocycler conditions were as follows: 1 cycle at 95°C for 1 minute; 40 cycles of 95°C for 30 sec, a annealing temperatures ranging from 40°C to 55°C for 30 seconds, and 72°C for 60 seconds; 1 cycle of 72°C for 5 minutes; and hold at 4°C for up to 4 hours or until the sample was transferred to the -20°C freezer.

DNA gel electrophoresis

A 1% gel was made by melting 0.5g agarose in 49mL of ddH_2O. Immediately after the solution was cooled, 1mL of 50XTAE and 2µL of ethidium bromide were added and swirled to mix. The agarose mixture was quickly poured into a sterilized 8x10cm gel tray with comb and left at room temperature for 45 minutes to allow the gel to solidify. The gel tray with attached comb was

placed in the 500mL of TAE running buffer in the gel box. The comb was removed by a vertical upward movement so as to not tear the wells. The GoTaq Green solution (Promega, WI, USA) used for PCR contained a loading buffer, so the samples were simply thawed by hand and the entire 20µL of sample was loaded into the gel. The DNA ladder was made by mixing 1µL of ladder (New England BioLabs, MA, USA), 2µL of 6XDNA loading buffer (New England BioLabs, MA, USA), and 9µL of ddH_2O. Gels were run at approximately 94V until the loading dye reached the bottom of the gel. The gel was then removed from the box and visualized under UV light.

Gel band extraction

Bands visualized under UV light were then removed from the gel using sterile razor blades and placed in Zymo-Spin IIIC column tubes (Zymo Research, CA, USA). Similar tissue types/band sizes were grouped together to maximize yield. The tubes were then centrifuged at 14,000rpm for 1 minute to allow the DNA to move through the column and collect at the base of the tube. The columns were discarded, but the DNA was stored at -20°C.

Band sequencing

The extracted bands were sequenced using a TOPO TA Cloning Kit for Sequencing (Invitrogen, NY, USA). 2.5µL of PCR product, 1µL of the dilute salt solution, 1µL TOPO vector, and 1.5µL autoclaved H_2O were mixed and incubated for 5 minutes at room temperature. 2µL of this solution was then added to electrocompetent *E. coli* cells. This mixture was then transferred to a 0.1cm cuvette and electroporated. Following the addition of 250µL of SOC medium, the solution was transferred to a 15mL Falcon tube and placed in a shaker for 1 hour at 37°C to allow the

expression of kanamycin-resistant genes. 5mL of plasmid and 20mL of SOC medium were then spread on kanamycin plate and allowed to incubate overnight at 37°C. Colonies were collected and cultured overnight in 24mL of LB broth. The plasmid was spun at max speed for 1 minute and the LB broth was decanted off. The plasmid was sequenced using a Zyppy Plasmid Miniprep Kit (Zymo Research, CA, USA. The bacteria were resuspended in 600µL of ddH_2O in a 1.5mL tube. 100µL of prewarmed 7X lysis buffer was added and the solution was inverted 5 times before incubating at room temperature for a maximum of 2 minutes. 350µL of cold neutralization buffer was added and the solution was mixed thoroughly before centrifugation at max speed for 4 minutes. Supernatant was transferred to a spin column in a collection tube and pulse spun for 15 seconds. Flow through was discarded before 200µL of endo-wash buffer was added to the column. Following a 30 second pulse spin, 400µL of Zyppy wash buffer was added and centrifuged again at max speed for 1 minute. To ensure all wash buffer had eluted from the column, the column was pulse spun for an additional 30 seconds. The column was then transferred to a clean 1.5 microcentrifuge tube and 30µL of Zyppy elution Buffer was added to the center of the column and incubated for 1 minute at room temperature. The column was then centrifuged for 30 seconds to elute the plasmid DNA. Sequencing PCR was completed using 1µL of M13 plasmid primer, 1.5µL plasmid DNA, 2.5µL autoclaved H_2O, and 2uL BigDye. Thermocycler conditions were as follows: 1 cycle at 96°C for 2 minutes; 32 cycles of 96 for 30 seconds, 39°C for 15 seconds, and 60°C for 4 minutes; indefinite hold at 4°C. The PCR product was carefully loaded into the center of the gelbed surface of a pre-spun spin-50 mini-column and spun at 1,000 rpm for 3 minutes. The column was vacuum-centrifuged for 30 minutes before the samples were processed at the Texas A&M Gene Technologies Laboratory.

Specific primer design

The sequence obtained from the PCR on the thyroid-enriched tissue was run through NCBI blast (http://blast.ncbi.nlm.nih.gov) to confirm its identity as NIS. This sequence was included in a multiple sequence alignment using Clustal X software. Based on this alignment, homologous red drum NIS primers were designed. The forward primer was GCTGTGATCTGGA CTGATGTGTTCCA and the reverse primer was TCCCGCTGTATGCACAGGCAAGAA.

Tissue specificity studies

Red drum specific primers for NIS were used for PCR in all tissues collected as outlined in the tissue collection section: thyroid, brain, opercular membrane, gill, kidney, muscle, anterior intestine, medial intestine, posterior intestine, stomach, and pyloric caeca. PCR was completed as outlined above. Thermocycler conditions were as follows: 1 cycle at 95°C for 1 minute; 32 cycles of 95°C for 30 sec, 58°C for 30 seconds, and 72°C for 60 seconds; 1 cycle of 72°C for 5 minutes; and hold at 4°C for up to 4 hours or until the sample was transferred to the -20°C freezer. The resulting PCR products were visualized using DNA gel electrophoresis.

Sterilization between samples

Mortar and pestles were sterilized between each use by soaking in 1% SDS for 30 minutes and 100% hydrogen peroxide for 30 minutes, followed by an ethanol wash. To ensure that sterilization was effective TRIzol reagent was spread along the surface of the mortar and pestle. It was then subjected to RNA extraction, RT-PCR, and PCR as outlined above. It was visualized through an agarose gel.

CHAPTER III

RESULTS

Thyroid tissue collection

Thyroid tissue was collected by first cutting through the gill arches and removing the entire lower jaw (Figure 1A). Next, the lower jaw was cut away (Figure 1B), resulting in the soft tissue ventral to and between the 2nd and 4th gill arches (Figure 1C). The gill arches were removed, leaving just soft, vascularized tissue. The gills arches were difficult to remove as the bones projected deep into the soft tissue. To aid in tissue homogenization and gill arch removal, the tissue was cut into smaller pieces before being snap frozen in liquid nitrogen. When collecting gill tissue samples and thyroid tissue samples, the thyroid samples were collected first. The removal of gill arches prior to thyroid dissection made it difficult to determine the location of the 2nd and 4th gill arches, complicating the thyroid tissue collection.

Figure 1 Thyroid tissue collection.

RNA yield and gel electrophoresis

Extracted RNA yield was calculated using Nanodrop technology and represented in Figure 2. A 260/280nm ratio of 1.8 was considered ideal for RNA samples, but any ratio between 1.5 and 2.0

was considered acceptable. Samples outside of this range most likely had phenols or proteins remaining from the RNA extraction. Three of the extracted gill RNA samples had very low yield and were not used for the study. This low yield was likely caused by the TRIzol-homogenate mixture clogging the pipette tip during the first step of the RNA extraction. To prevent clogging in the rest of the samples, a sterile razor blade was used to cut off the pipette tip to create a larger opening. RNA extractions from all three regions of the intestine resulted in a yellow aqueous layer compared to all other samples with a clear aqueous layer. However, this did not affect 260/280 ratios and yield.

Figure 2 – RNA Extraction Results

Tissue	260/280 ratio	RNA Yield (ng/µL)
Gill 1 (G1)	1.76	9.0*
Gill 2 (G2)	2.09**	12.5*
Gill 3 (G3)	1.76	122.5
Gill 4 (G4)	1.83	43.5*
Gill 5 (G5)	1.94	813.2
Gill 6 (G6)	1.94	3250.1
Gill 7 (G7)	1.96	1289.2
Gill 8 (G8)	1.90	499.3
Thyroid 1	1.88	360.6
Thyroid 2	1.88	130.8
Thyroid 3	1.78	327.5
Thyroid 4	1.81	272.9
Brain 1	1.65	3149.7
Brain 2	1.55	1058.7
Brain 3	1.07**	4433.3
Brain 4	1.75	336.8
Opercular Mem. 1	1.57	1625.2
Opercular Mem. 2	1.51	553.5
Kidney	1.53	583.7
Muscle	1.67	957.2
Anterior Intestine 1	1.66	860.5
Anterior Intestine 2	1.61	806.2
Medial Intestine 1	1.77	694.6
Medial Intestine 2	1.69	661.9

Figure 2 – RNA Extraction Results (Continued**)**

Tissue	260/280 ratio	RNA Yield (ng/µL)
Posterior Intestine 1	1.61	949.1
Posterior Intestine 2	1.95	400.3
Stomach 1	1.79	1852.9
Stomach 2	1.76	1717.9
Pyloric Caecum 1	1.73	1928.3
Pyloric Caecum 2	1.90	986.7

Legend: * indicates an RNA yield too low for use; ** indicates a 260/280 ratio outside of the accepted range.

RNA integrity was tested to verify that the methodology used would result in satisfactory RNA. RNA integrity was judged based on formaldehyde RNA gel electrophoresis (Figure 3) for a representative tissue, the gill. Any of the extracted samples could have been used, but gill samples were used because gill was an easily accessible tissue that could be collected quickly. RNA integrity was determined by the presence of singular, intact ribosomal subunit bands with no smearing. The RNA gel showed that the remaining gill RNA samples were undegraded, verifying that the tissue homogenization and RNA extraction process was not diminishing the integrity of the RNA.

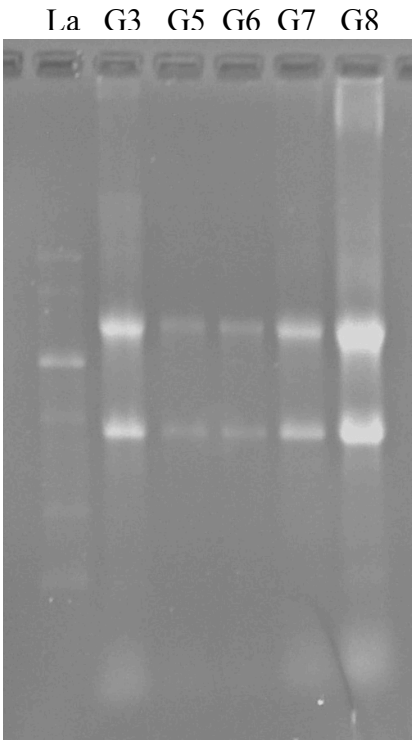

Figure 3 RNA gel showing RNA integrity based on the relatively tight bands located at the size of the ribosomal subunits. Legend: La, ladder; G3, gill sample 3; G5, gill sample 5; G6, gill sample 6; G7, gill sample 7; G8, gill sample 8.

Degenerate primer design

A multiple sequence alignment using Clustal X software was used to align all known NIS gene sequences (Figure 4). Partial sequences that did not extend into the highly conserved regions were deleted from the alignment in order to better observe the base pairs that were conserved, represented by stars in the top row of the alignment. Using this alignment, the forward NIS primer was chosen to be ATT$^{C}_{T}$T$^{G}_{C}$AA$^{C}_{T}$CAAG$^{C}_{T}$NACNGG and the reverse NIS primer was GCCATNGC$^{G}_{A}$TT$^{G}_{A}$AT$^{G}_{A}$CTNGT$^{G}_{A}$GA.

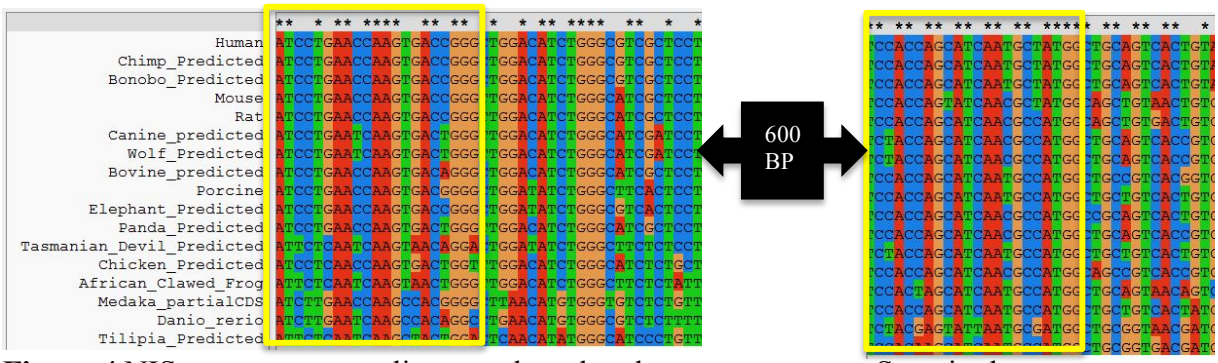

Figure 4 NIS gene sequence alignment based on known sequences. Stars in the top row represent 100% conservation between species at that base pair. The base pairs are color-coded for visual comparison: A, red; G, orange; C, blue; T, green. The yellow boxes surround the region chosen for forward and reverse primers, respectively.

Thyroid NIS expression

Using these degenerate primers an amplified product of approximately 600bp was expected. Thyroid samples 1 and 2 (Figure 2) were combined to increase yield in order to obtain the 2µg of RNA needed to complete RT-PCR. Gill sample 6 was also used. The PCR thyroid-enriched tissue and gill tissue was run three separate times with annealing temperatures of 40C, 50C, and 55C. A band of roughly 600bp was amplified from the thyroid samples run with annealing temperatures of 55C and 50C (Figure 5). Bands at approximately 400bp from the gill and thyroid samples run at 40C and 50C were also present. The 600bp band present in the thyroid samples was cut from the gel, sequenced, and confirmed to be NIS by BLAST analysis. The 400bp band was determined to be the 19S ribosomal subunit.

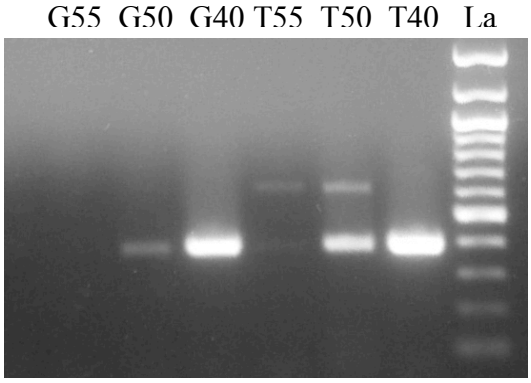

Figure 5 DNA gel showing proposed NIS amplification in red drum thyroid tissue using annealing temperatures of 50C and 55C. Legend: G55, gill with annealing temp of 55C; G50, gill with annealing temp of 50C; G40, gill with annealing temp of 40C; T55, thyroid with annealing temp of 55C; T50, thyroid with annealing temp of 50C; T40, thyroid with annealing temp of 40C; La, ladder.

Specific NIS Primers

Using the partial sequence obtained from the 600 bp gel band from the thyroid-enriched tissue, red drum NIS specific primers were designed using Clustal X software. The forward primer was GCTGTGATCTGGA CTGATGTGTTCCA and the reverse primer was TCCCGCTGTATGCACAGGCAAGAA.

NIS mRNA tissue specificity

The homologous red drum NIS primers were used to amplify NIS DNA from a variety of red drum tissues to identify locations of greatest expression. Samples were originally run separately on different gels grouped by related tissues. However, when running a final set of gels with all samples trouble arose. Contamination was repeatedly observed in the no template controls and in samples that had previously been negative. Equipment was bleached and new PCR ingredients were used to effectively remove this contamination before running final gels. The final DNA gels (Figure 6) are presented along with the original expectation for each tissue based on the literature review presented in the Introduction (Figure 7). NIS expression was found in red drum

thyroid, gill, intestine, pyloric caeca, and brain. No expression was found in red drum opercular membrane, stomach, kidney, and muscle.

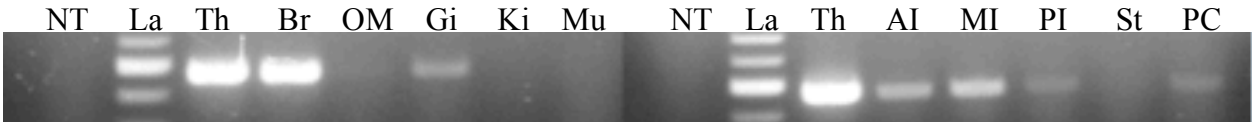

Figure 6 DNA gel showing tissue-specific expression of NIS in indicated red drum tissues. Legend: NT, no template; La, ladder; Th, thyroid; Br, brain; OM, opercular membrane; Gi, gill; Ki, kidney; Mu, muscle; AI, anterior intestine; MI, medial intestine; PI, posterior intestine, St, stomach; PC, pyloric caeca.

Figure 7 – NIS Tissue Specificity Based on RT-PCR

Tissue	Hypothesis	Result
Thyroid	+	+
Brain	-	+
Opercular Membrane	+	-
Gill	+	+
Kidney	+	-
Muscle	-	-
Anterior Intestine	+	+
Medial Intestine	+	+
Posterior Intestine	+	+
Stomach	+	-
Pyloric Caeca	+	+

CHAPTER IV

DISCUSSSION AND CONCLUSIONS

Thyroid hormones are essential to many physiological processes and their synthesis is dependent on the presence of iodine in the thyroid. In mammals, thyroid hormone synthesis is dependent on uptake of iodine from the blood into thyroid tissue by the NIS, with diet being the ultimate iodide source (Nicola et al, 2009; Zimmerman, 2009, Dohan et al., 2003). In contrast, it has been proposed that fish can obtain iodide directly from their environment by pumping it across gills (Eales, 1979; Hunn and Fromm, 1996). My study was designed to determine whether fish possess both gill and gut iodide uptake mechanisms by characterizing NIS mRNA expression in various tissues of the red drum. I first hypothesized that NIS mRNA would be expressed in thyroid-enriched tissue of red drum, where it should function to transport iodine from the blood to thyrocytes for thyroid hormone synthesis. Next I looked for NIS mRNA expression in putative environmental iodine transporting tissues, including gill, opercular membrane, stomach, pyloric caeca, intestine, and kidney. Brain and muscle were included as negative controls and were not expected to express NIS.

My tissue homogenization technique using liquid nitrogen with a mortar and pestle was a new to our lab and was adopted because of the need to extract RNA from complex tissue samples containing bone and other connective tissues. It successfully enabled homogenization of larger and tougher tissues, such as the gill and thyroid-enriched tissue. When working with the mortar and pestle for longer periods of time on the tougher tissues multiple pairs of cryogenic gloves were needed. As the gloves became damp and cold they were switched out for fresh, dry gloves.

Despite these difficulties, I propose that liquid nitrogen homogenizations continue to be used in future studies for larger tissues. This technique was successful for obtaining high RNA yields from the complete homogenization of tissues containing bones.

I chose to use the TRIzol method for RNA extraction over a commercially available RNA extraction kit. TRIzol typically results in a higher RNA yield which was necessary for some of the more difficult to homogenize tissues. While TRIzol can be dangerous to work with, the resulting RNA quality and yield was excellent and the protocol was quick and simple. The DNase treatment, reverse transcription, and PCR techniques outlined in the methods were performed according to manufacturer's protocols. No problems arose with the RNA extraction, DNase treatment, or reverse transcription. During the final rounds of PCR and gel electrophoresis, several control samples became contaminated. Several gels were excluded from the results as the no template control was positive. New primer stock and PCR ingredient stock was used; however, this didn't resolve the contamination problem. Pipettes were then disassembled and bleached to remove possible contamination. In the end, another lab's thermocycler was used for the final PCR reactions presented in Figure 6 in which there were no bands in the no template controls. While we are still uncertain, we hypothesize that our thermocycler lid is not clamping down tightly enough, possibly leading to cross contamination between PCR tubes. Despite the contamination problems, I am confident in the final results of the gel presented. The positive signals for NIS gene expression were consistent across all gels, even those with contamination.

My observation of NIS expression in the thyroid confirms the hypothesis that the symporter is

structurally conserved in teleost fish and suggests its functional importance in thyroid hormone synthesis in fish. Because I obtained only a partial NIS sequence for red drum, we do not yet know how closely the complete gene structure or protein structure resemble those in other vertebrate species. However, the well established expression of NIS in mammalian thyroid (Nicola et al, 2009; Zimmerman, 2009, Dohan et al., 2003; Ferreira et al, 2010) as well as in four species of fish thyroid (Carr et al, 2008) suggest that it has been conserved in its thyroid tissue distribution for at least 250 million years.

Eales (1979) and Hunn and Fromm (1996) proposed that teleost fish possess an iodine transport mechanism in their gills. Using degenerate primers and RT-PCR I was unable to amplify NIS from gill tissue mRNA, but I was able to detect significant NIS expression from gill filaments using homologous primers. Although the RT-PCR technique I used was not designed to be quantitative, this does suggest that while the NIS is expressed in gill tissue, it may be at very low levels. It is also possible that the temperatures used in the PCR reaction with degenerate primers were not optimally suitable for NIS amplification from gill tissue. Expression in the gills suggests that the previously proposed branchial iodide pump might actually be the NIS. In contrast, whereas the opercular membrane is known to contain ion transporters (Degnan and Zadunaisky, 1979), no NIS expression was found in this tissue.

In mammals, the intestine is the primary location of iodine absorption from the environment (Nicola et al, 2009; Zimmerman, 2009, Dohan et al., 2003). Like mammals, the NIS is expressed in all three regions of the intestine of red drum. The pyloric caeca have known involvement in water and nutrient absorption (Boge et al, 1988). Due to this, and the established presence of NIS

in other areas of the digestive tract, I expected that the NIS might be expressed in the pyloric caeca, which was confirmed. NIS expression in fish stomach has not been studied Stomach was also included in the present study as part of the digestive tract and also hypothesized to express NIS. However, no expression was found, suggesting the stomach is not able to transport iodide. Spitzweg et al (1998) and Dohan et al (2003) found NIS expression in human gastric mucosa, but noted that expression levels varied greatly between individuals. This suggests that gastric NIS expression might exist in fish under different physiological or environmental conditions. The kidney, like the opercular membrane, is a tissue known for ion transport (Stokes, 1982). Spitzweg et al (2001) demonstrated NIS expression in human kidney confirmed by RT-PCR and western blotting. However, no NIS expression was found in the kidney in my study. One possible explanation for the lack of kidney expression is insufficient tissue collection. The red drum kidney is a difficult tissue to remove cleanly. Kidney tissue collection was done by scraping tissue from the dorsal body wall of the peritoneal cavity of red drum. It is possible that few kidney cells were obtained by this scraping or that the parts of the kidney collected by this scraping did not express NIS.

Muscle and brain tissues were both included as negative controls, as neither were expected to express the NIS gene. This was confirmed in muscle tissue. Perhaps the most interesting outcome of this tissue specificity study was the strong NIS expression in the brain. Perron et al (2001) found minimal NIS expression in the brain of rats but had no explanation as to its function. Based on a radioiodine study in mice Engstrom et al (1984) hypothesized that iodine passively crosses the epithelial cells of the blood-brain-barrier into the cerebrospinal fluid, but that the NIS is needed to actively transport iodide out of the CSF, possibly in the choroid plexus.

NIS expression in the brain of red drum warrants further studies to localize it to specific regions in hopes of discovering a novel function of the NIS in the central nervous system of fish.

In conclusion, I have shown that homologous primers can be used to identify NIS mRNA expression in red drum tissues. Finding NIS expression in the gills and intestines suggests multiple pathways for iodide accumulation and provides new directions for studies of iodide utilization in teleost fish. Demonstration of NIS expression both the gills and gut suggests that both branchial and gastrointestinal mechanisms of iodine absorption exist in this fish. Confirmation of this hypothesis will require further studies of the physiological regulation of these symporters, as well as biochemical characterization of the enzyme function. Future physiological studies should examine symporter expression levels using more sensitive quantitative PCR techniques as the results of the end point PCR techniques I used cannot be used to draw quantitative conclusions on expression levels. While brightness of bands is a good indicator of the amount of expression, q-PCR is needed to provide quantifiable, conclusive data. Additionally, identifying expression locations in gills and intestine, utilizing techniques such as *in situ* hybridization, can help establish the functional significance of this protein under differing conditions of iodine availability. Because freshwater and saltwater fish regulate water and ion absorption differently, it would be interesting to undertake a comparative study of NIS gene expression in fish held in different salinities and iodine concentrations. Gill NIS expression may be of greater importance in fish held in low iodine environments. Understanding these pathways of iodide uptake can help to better establish dietary and environmental iodide levels for aquaculture species, as well as help to understand the effects of variable environmental iodide on endocrine systems important for growth and development of teleost fish.

REFERENCES

Boge, G., Lopez, L, Peres, G. (1988). An in vivo study of the role of pyloric caeca in water absorption in rainbow trout (*Salmo gairdneri*). *Comparative Biochemistry and Physiology.* 91(1): 9-13.

Carr, D.L., Carr, J.A., Willis, R.E., Pressley, T.A. (2008). A perchlorate sensitive iodide transporter in frogs. *General and Comparative Endocrinology*. 156(1), 9-14.

Degnan, KJ. & Zadunaisky J.A. (1979). Open-circuil sodium and chloride fluxes across isolated opercular epithelia from the teleost Fundulus herteroclitus. *Journal of Physiology*, 294(1), 483-495.

Dohan, O., De la Vieja, A., Paroder, V., Reidel, C., Artani, M., Reed, M., Ginter, C.S., Carrasco, N. (2003). The sodium/iodide symporter (NIS): Characterization, regulation, and medical significance. *Endocrinology Review*, 24(1), 48-77.

Eales, J. G. (1979). Thyroid functions in cyclostomes and fishes. In E. Barrington, *Hormones and Evolution* (Vol. 1). New York, NY: Academic Press.

Engstrom, L., Chow, S., Kemp, J.W., Woodbury, D.M. (1984). Radioiodide uptake in brain, CSF, thyroid, and salivary glands of audiogenic seizure mice. *Epilepsia*. 25(4): 518-525.

Ferreira, A.C., Lima, L.P., Araujo, R.L., Muller, G., Rocha, R.P., Rosenthal, D., Carvalho, D.P. (2010). Rapid regulation of thyroid sodium–iodide symporter activity by thyrotrophin and iodine. *Journal of Endocrinology,* 184**,** 69–76.

Gregory, L.A. & Eales, J.G. (1975). Factors contributing to high levels of plasma iodide in brook trout, *Saluelinus fontinalis* (Mitchill). *Canadian Journal of Zoology*, 53, 267-277.

Hadley, M.E. & Levine, J.E. (2007). *Endocrinology.* (6th ed). New Jersey: Pearson Prentice Hall.

Higgs, D.A., Fagerlund, U.H., Eales, J.G., McBride, J.R. (1982). Application of thyroid and steroid hormones as anabolic agents in fish culture. *Comparative Biochemistry and Physiology*, 73B(1), 143-176.

Hunn, J.B. & Fromm, P.O. (1966). In vivo uptake of radioiodide by rainbow trout. *Water Pollution Control Federation*, 38(12), 1981-1985.

Kerstetter, T.H., Kirschner, L.B., Rafuse, D.D. (1970). On the mechanisms of sodium ion transport by the irrigated gills of rainbow trout (*Salma gairdneri*). *Journal of General Physiology,* 56(3), 342-359.

Kupper, F.C., Feiters, M.C., Olofsson, B., Kaiho, T., Yanagida, S., Zimmerman, M,B.,

Carpenter, L.J., Kuther, G.W., Lu, Z., Jonsson, M., Kloo, L. (2011). Commemorating two centuries of iodine research: An interdisciplinary overview of current research. *Angwandte Interdisciplinary Chemistry*. 50, 11598-11620.

Nicola, J.P., Basquin, C., Portulano, C., Reyna-Neyra, A., Paroder, M., Carrasco, N. (2009). The NA+/I- symporter mediates active iodide uptake in the intestine. *American Journal of Physiology-Cell Physiology*, 296, 654-662.

Perron B, Rodriguez AM, Leblanc G, Pourcher T. (2001) Cloning of the mouse sodium iodide symporter and its expression in the mammary gland and other tissues. *Journal of Endocrinology*. 170:185–196

Spitzweg, C., Dutton, C.M., Castro, M.R., Bergert, E.R., Goellner, J.R., Heufelder, A.E., Morri, J.C. (2001). Expression of the sodium iodide symporter in human kidney. *Kidney International.* 59: 1013-1023.

Spitzweg, C., Joba, W., Eisenmenger, W., Heufelder, A.E. (1998). Analysis of human sodium iodide symporter gene expression in extrathyroidal tissues and cloning of its complementary deoxyribonucleic acids from salivary gland, mammary gland, and gastric mucosa. *The Journal of Clinical Endocrinology and Metabolism*. 83(5): 1746-1751.

Stokes, J.B. (1982). Ion transport by the cortical and outer medullary collecting tubule. *Kidney International*. 22: 473-484.

Taurog, A. & Chaikoff, I.L. (1948). The nature of circulating thyroid hormone. *The Journal of Biological Chemistry*, 176, 639-656.

Wantabe, T., Kiron, V., Satoh, S. (1997). Trace minerals in fish nutrition. *Aquaculture*, 151, 185-207.

Zhand, S., Schwehr, K.A., Ho, Y.F., Xu, C., Roberts, K.A., Kaplan, D.I., Brinkmeyer, R., Yeager, C.M., Santschi, P.H. (2010). A novel approach for the simultaneous determination of iodide, iodate, and organo-iodide for ^{127}I and ^{129}I in environmental samples using gas chromatography-mass spectrometry. *Environmental Science and Technology*, 44, 9042-9048.

Zimmerman, M.B. (2009). Iodine Deficiency. *Endocrine Reviews,* 30(4), 376–408.